Supporting Information

A miniaturized, battery-free, wireless wound monitor that predicts wound closure rate early

Nate T. Garland, Joseph W. Song, Tengfei Ma, Yong Jae Kim, Abraham Vázquez-Guardado, Ayemeh Bagheri Hashkavayi, Sankalp Koduvayur Ganeshan, Nivesh Sharma, Hanjun Ryu, Min-Kyu Lee, Brandon Sumpio, Margaret A. Jakus, Viviane Forsberg, Rajaram Kaveti, Samuel K. Sia, Aristidis Veves, John A. Rogers, Guillermo A. Ameer, Amay J. Bandodkar

*Corresponding authors: Amay J. Bandodkar, ajbandod@ncsu.edu;
Guillermo A. Ameer, g-ameer@northwestern.edu;
John A. Rogers, jrogers@northwestern.edu

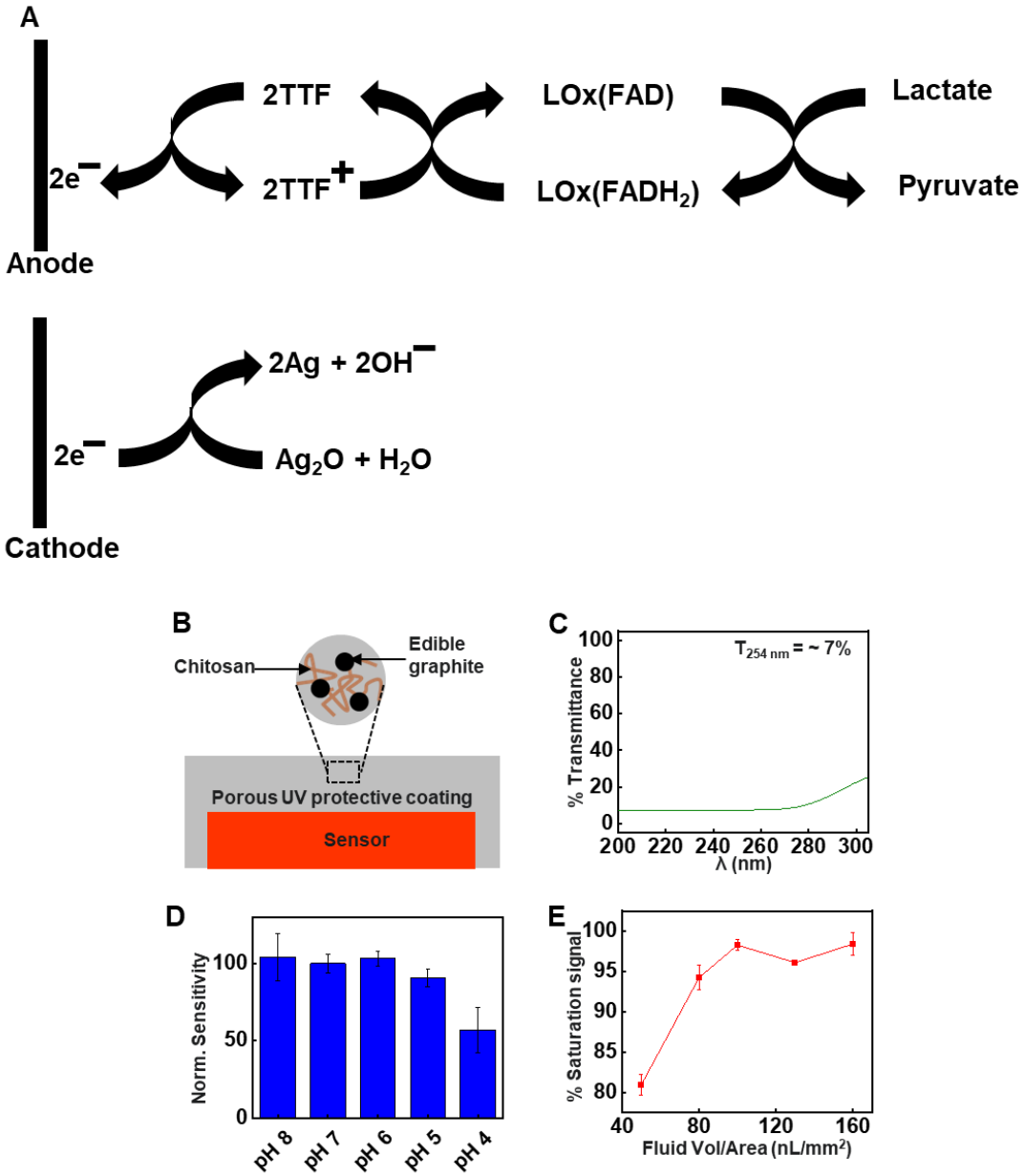

Figure S1. (A) Schematic representation of the reactions occurring at the biofuel cell-based lactate sensor. (B) Scheme showing UV protective coating layer over the lactate sensor. (C) UV transmittance spectrum for the UV protective coating. (D) Effect of pH on sensor sensitivity. (E) Percent saturation signal as a function of fluid volume per surface area of a phantom wound. (D,E) Data presented as mean ± S.D., n=3.

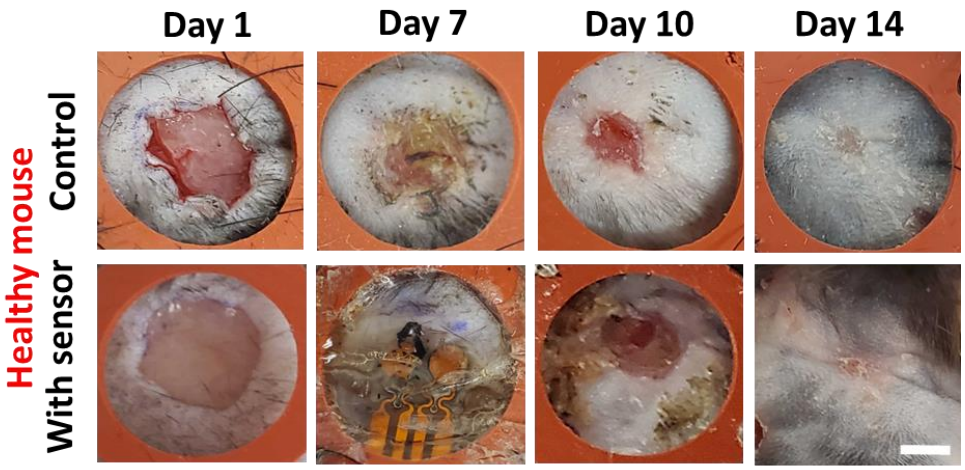

Figure S2. Effect of the sensor on long-term wound closure process. Scale bar: 2.5 mm.

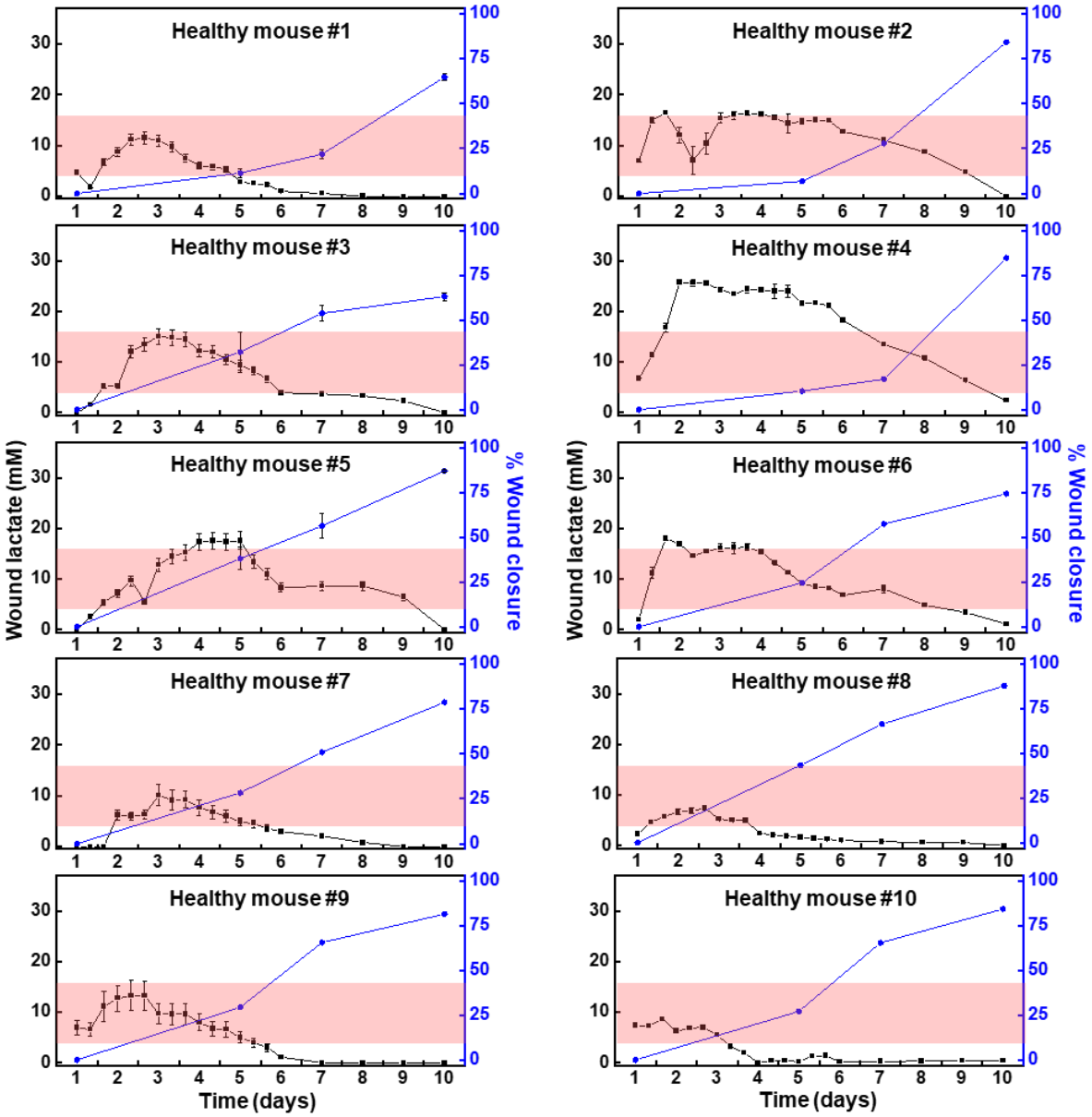

Figure S3. Individual plots for measured lactate level and % wound closure for each healthy mouse. Pink region represents healthy wound lactate range. Data presented as mean ± S.D., n=60.

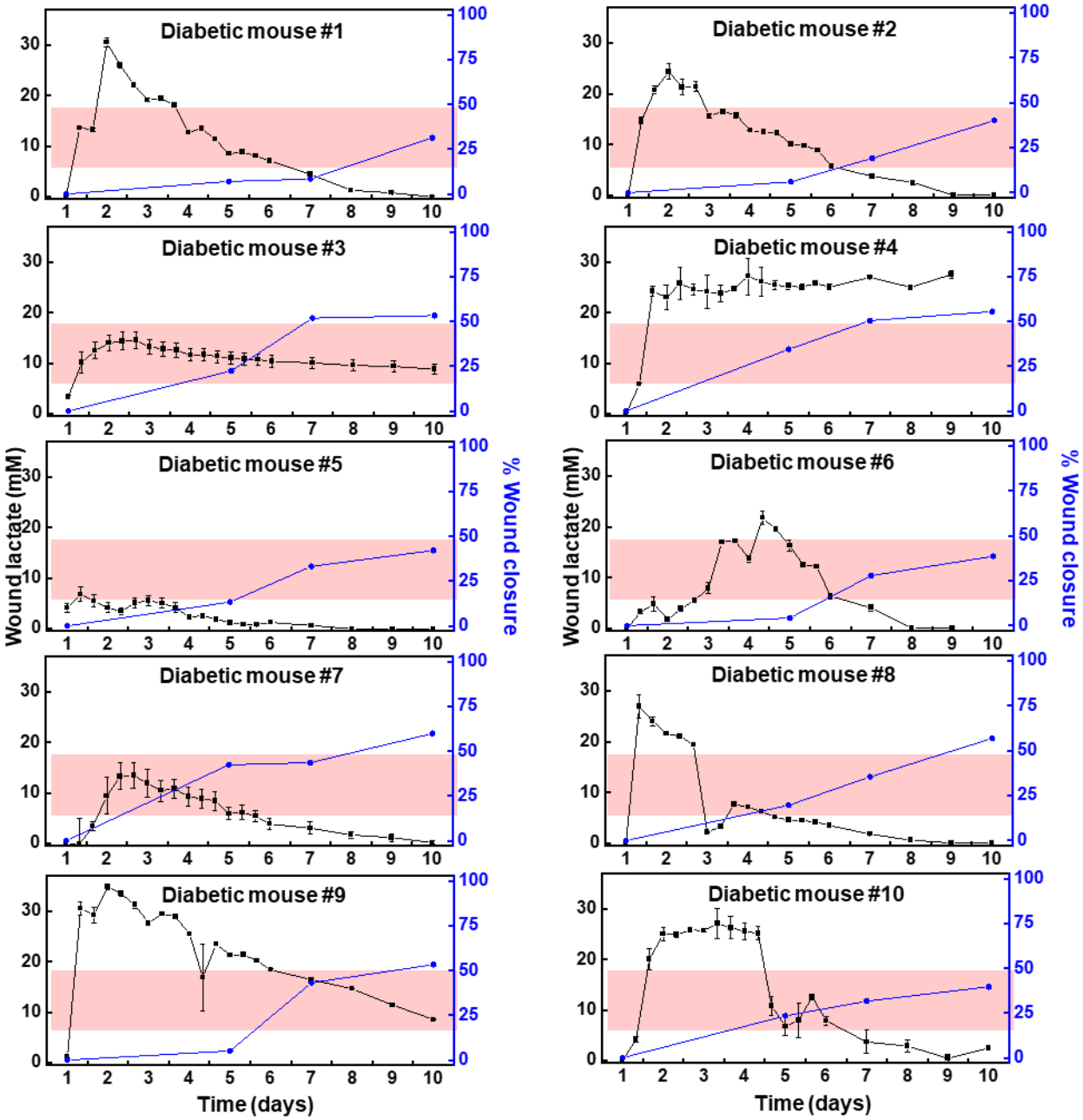

Figure S4. Individual plots for measured lactate level and % wound closure for each diabetic mouse. Pink region represents healthy wound lactate range. Data presented as mean ± S.D., n=60.

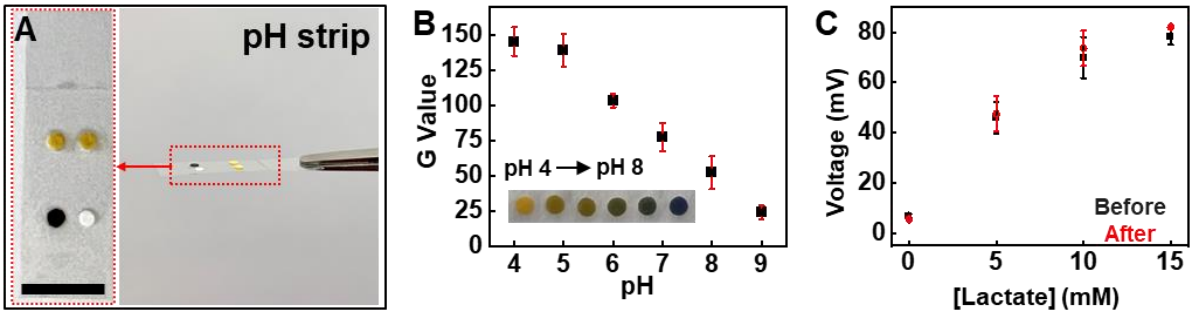

Figure S5. (A) Image of the pH strip. Scale bar 5 mm. (B) Calibration plot for the pH assays (data presented as mean ± S.D., n=4). (C) Data demonstrating the ability of the lactate sensor to perform in constricted body regions subjected to cyclical and continuous loading. The study involves applying three sensors to the heel of a healthy human subject (male; weight: 70 kg). The heel is selected as the region of interest due to its high risk of developing chronic wounds. The subject continuously walks for 30 min followed by standing still for 15 min. Data presented as mean ± S.D., n=60.

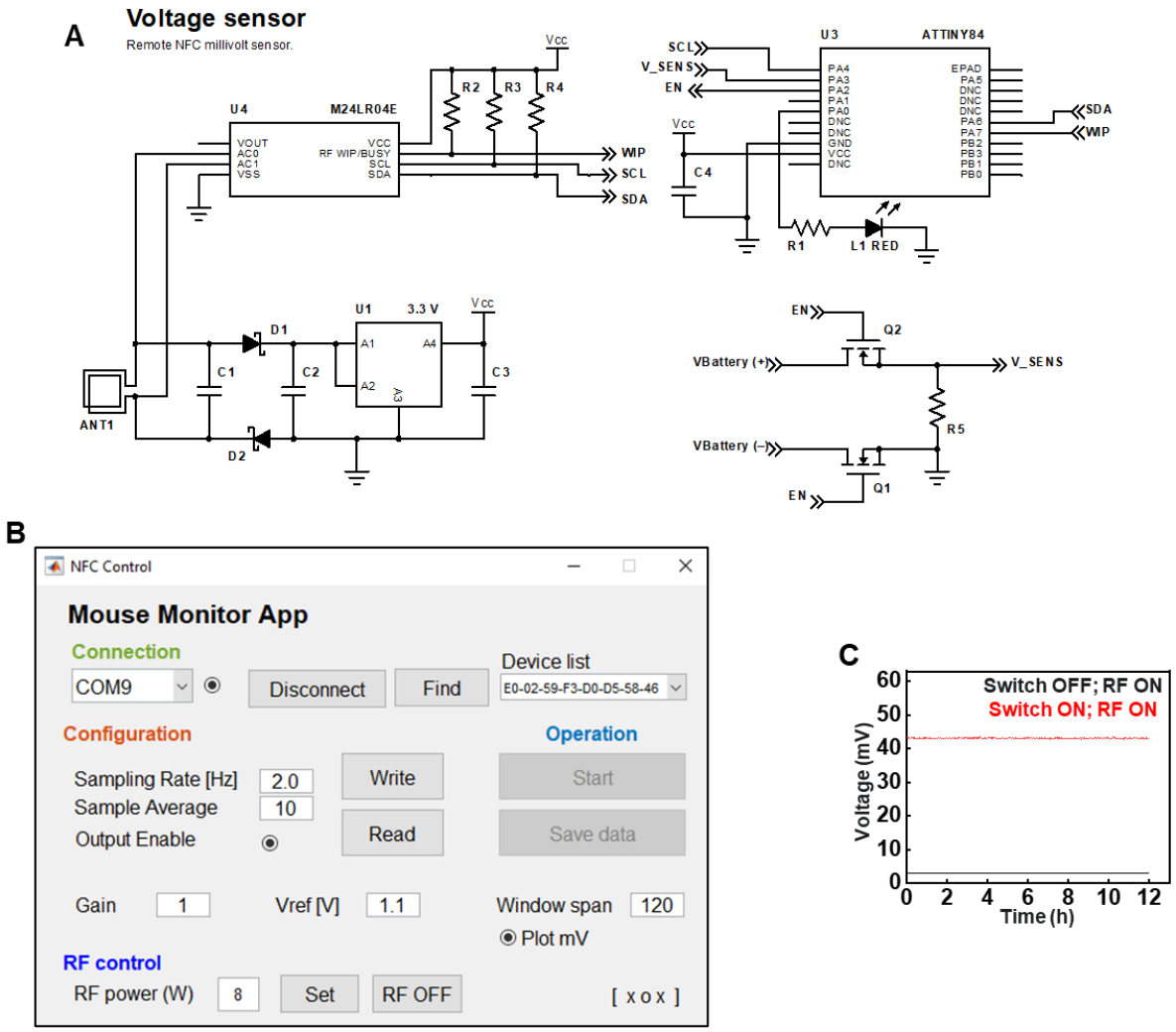

Fig. S6. (A) Detailed circuit design of wireless electronics. (B) Screenshot of the GUI for data acquisition. (C) Effectiveness of the MOSFET switch to electronically couple the sensor to wireless electronics only during data acquisition period.

Table S1: Comparison of present work with some representative examples of wound monitors published since year 2020.

Wound parameters measured	In vivo model	Additional features	Wound closure prediction	Data transmission	Power source	Footprint	Ref.
Temperature	Mini pig	UV-triggered gentamicin antibiotic applied to wound based on wound temperature	No	Bluetooth	Battery	*15 cm^2	[1]
pH, uric acid, lactate, temperature, ammonium, glucose	Diabetic rat	Electrical stimulation electrodes, iontophoretic delivery of c-terminal peptide-25	No	Bluetooth	Battery	*11 cm^2	[2]
Cathepsin, humidity, pH, temperature	Mouse	Electrical stimulation electrodes, wound healing photothermal IR LED	No	Bluetooth	Battery	* 32 cm^2	[3]
Tumor necrosis factor–a, interleukin-6 (IL-6), IL-8, transforming growth factor–b1, microbial burden (Staphylococcus aureus), temperature, pH	Mouse	-	No	Bluetooth	Battery	* 89 cm^2	[4]
DNA from parthenogenic bacteria in wounds	Mouse	-	No	NFC	Battery free sensing, power source required for data transmission	* 2 cm^2	[5]
Wound impedance	Mouse	Electrical stimulation electrodes	No	NFC	NFC wireless power transfer	* 3 cm^2	[6]
Wound impedance, temperature	Mouse	Electrical stimulation electrodes, temperature reversible skin adhesion	No	NFC	Radio frequency energy harvesting	* 20 cm^2	[7]
Sodium, potassium, calcium, pH, uric acid, and temperature	Rat	-	No	Bluetooth	Battery	* 10 cm^2	[8]
pH	Human wounds	-	Yes	RFID	Passive electronics	* 13 cm^2	[9]
Temperature, strain, glucose	Diabetic mouse	Zwitterionic hydrogel to promote wound healing	No	Wired	Externally powered	* 2.4 cm^2	[10]

Wound parameters measured	In vivo model	Additional features	Wound closure prediction	Data transmission	Power source	Footprint	Ref.
Temperature, uric acid, pH	Rat	Cefazolin antibiotic drug delivery electrodes	No	NFC	NFC wireless power transfer	10 cm^2	[11]
Temperature, pH, trimethylamine, uric acid, moisture	Rat	-	No	Smartphone image capture	None, colorimetric assay	3.24 cm^2	[12]
Lactate	Diabetic mouse / healthy mouse	-	Yes	NFC	Self-powered biofuel cell sensor	1.7 cm^2	This work

*: estimated

References

[1] Q. Pang, D. Lou, S. Li, G. Wang, B. Qiao, S. Dong, L. Ma, C. Gao, Z. Wu, *Adv. Sci.* **2020**, *7*, 1902673.

[2] E. Shirzaei Sani, C. Xu, C. Wang, Y. Song, J. Min, J. Tu, S. A. Solomon, J. Li, J. L. Banks, D. G. Armstrong, W. Gao, *Sci. Adv.* **2023**, *9*, eadf7388.

[3] S. M. Yang, H. Kim, G. Ko, J. C. Choe, J. H. Lee, K. Rajaram, B. An, W. B. Han, D. Kim, J. Shin, T. Jang, H. Kang, S. Han, K. Lee, S. J. Oh, S. Hwang, *Nano Today* **2022**, *47*, 101685.

[4] Y. Gao, D. T. Nguyen, T. Yeo, S. B. Lim, W. X. Tan, L. E. Madden, L. Jin, J. Y. K. Long, F. A. B. Aloweni, Y. J. A. Liew, M. L. L. Tan, S. Y. Ang, S. D. /. Maniya, I. Abdelwahab, K. P. Loh, C. Chen, D. L. Becker, D. Leavesley, J. S. Ho, C. T. Lim, *Sci. Adv.* **2021**, *7*, eabg9614.

[5] Z. Xiong, S. Achavananthadith, S. Lian, L. E. Madden, Z. X. Ong, W. Chua, V. Kalidasan, Z. Li, Z. Liu, P. Singh, H. Yang, S. P. Heussler, S. M. P. Kalaiselvi, M. B. H. Breese, H. Yao, Y. Gao, K. Sanmugam, B. C. K. Tee, P. Chen, W. Loke, C. T. Lim, G. S. H. Chiang, B. Y. Tan, H. Li, D. L. Becker, J. S. Ho, *Sci. Adv.* **2021**, *7*, eabj1617.

[6] J. W. Song, H. Ryu, W. Bai, Z. Xie, A. Vázquez-Guardado, K. Nandoliya, R. Avila, G. Lee, Z. Song, J. Kim, M. Lee, Y. Liu, M. Kim, H. Wang, Y. Wu, H. Yoon, S. S. Kwak, J. Shin, K. Kwon, W. Lu, X. Chen, Y. Huang, G. A. Ameer, J. A. Rogers, *Sci. Adv.* **2023**, *9*, eade4687.

[7] Y. Jiang, A. A. Trotsyuk, S. Niu, D. Henn, K. Chen, C. Shih, M. R. Larson, A. Mermin-Bunnell, S. Mittal, J. Lai, A. Saberi, E. Beard, S. Jing, D. Zhong, S. R. Steele, K. Sun, T. Jain, E. Zhao, C. R. Neimeth, W. G. Viana, J. Tang, D. Sivaraj, J. Padmanabhan, M. Rodrigues, D. P. Perrault, A. Chattopadhyay, Z. N. Maan, M. C. Leeolou, C. A. Bonham, S. H. Kwon, H. C. Kussie, K. S. Fischer, G. Gurusankar, K. Liang, K. Zhang, R. Nag, M. P. Snyder, M. Januszyk, G. C. Gurtner, Z. Bao, *Nat. Biotechnol.* **2023**, *41*, 652.

[8] Z. Liu, J. Liu, T. Sun, D. Zeng, C. Yang, H. Wang, C. Yang, J. Guo, Q. Wu, H. Chen, X. Xie, *ACS Sens.* **2021**, *6*, 3112.

[9] S. Kalasin, P. Sangnuang, W. Surareungchai, *Anal. Chem.* **2022**, *94*, 6842.

[10] H. Guo, M. Bai, Y. Zhu, X. Liu, S. Tian, Y. Long, Y. Ma, C. Wen, Q. Li, J. Yang, L. Zhang, *Adv. Funct. Mater.* **2021**, *31*, 2106406.

[11] G. Xu, Y. Lu, C. Cheng, X. Li, J. Xu, Z. Liu, J. Liu, G. Liu, Z. Shi, Z. Chen, F. Zhang, Y. Jia, D. Xu, W. Yuan, Z. Cui, S. S. Low, Q. Liu, *Adv. Funct. Mater.* **2021**, *31*, 2100852.

[12] X. T. Zheng, Z. Yang, L. Sutarlie, M. Thangaveloo, Y. Yu, N. A. B. M. Salleh, J. S. Chin, Z. Xiong, D. L. Becker, X. J. Loh, B. C. K. Tee, X. Su, *Sci. Adv.* **2023**, *9*, eadg6670.